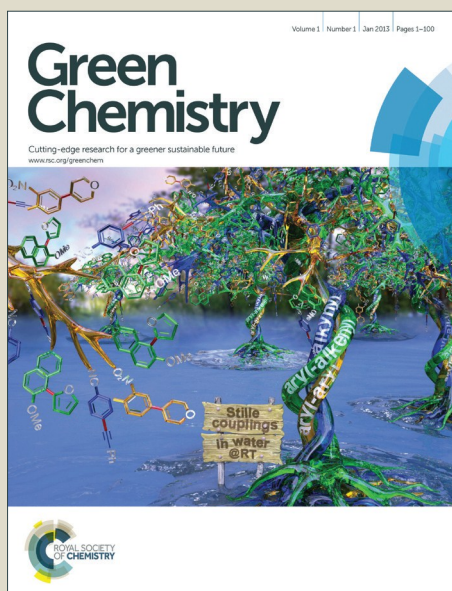


Green Chemistry

Accepted Manuscript



This is an *Accepted Manuscript*, which has been through the Royal Society of Chemistry peer review process and has been accepted for publication.

Accepted Manuscripts are published online shortly after acceptance, before technical editing, formatting and proof reading. Using this free service, authors can make their results available to the community, in citable form, before we publish the edited article. We will replace this *Accepted Manuscript* with the edited and formatted *Advance Article* as soon as it is available.

You can find more information about *Accepted Manuscripts* in the [Information for Authors](#).

Please note that technical editing may introduce minor changes to the text and/or graphics, which may alter content. The journal's standard [Terms & Conditions](#) and the [Ethical guidelines](#) still apply. In no event shall the Royal Society of Chemistry be held responsible for any errors or omissions in this *Accepted Manuscript* or any consequences arising from the use of any information it contains.



www.rsc.org/greenchem

ARTICLE

Sonochemical Synthesis of HSiW/Graphene Catalyst for Enhanced Biomass Hydrolysis

Cite this: DOI: 10.1039/x0xx00000x

Miri Klein,^a Alexander Varvak,^b Elad Segal,^a Boris Markovsky,^a Indra Neel Pulidindi,^a Nina Perkas^a and Aharon Gedanken^{*a,c}

Received 00th October 2014,
Accepted 00th January 2012

DOI: 10.1039/x0xx00000x

www.rsc.org/

Hydrolysis of glycogen for the production of glucose was studied. Silicotungstic acid (HSiW), was deposited on graphene by an ultrasound-assisted procedure. The catalyst (HSiW/G) was characterized using a variety of physico-chemical methods. Homogeneous distribution of HSiW on the surface of graphene was demonstrated. The hydrolysis of glycogen was performed with HSiW/G catalyst by hydrothermal treatment. The yield of glucose (66 wt. %) obtained was about 8 times higher than that obtained with the same amount of bare HSiW. Stability of the HSiW/graphene even after 3 repeated uses was confirmed. The mechanism of the enhancement of catalytic activity was discussed in terms of special interaction between the graphene support and HSiW and also the appearance of hydrophobic cavities on the surface of graphene. The formation of these cavities facilitate the anchoring of glycogen to the catalyst surface and promote the attack of protons that leads to selective, rapid, and efficient hydrolysis.

Introduction

Current energy systems are based mainly on fossil resources such as coal, petroleum and natural gas. However, the rapid consumption of natural resources prompts research to find renewable energy sources to meet increasing demand [1].

Biomass is a sustainable source of organic carbon, which is considered as part of the solution to produce biofuels and chemicals [2, 3]. Biomass is obtainable world-wide in the form of organic materials such as grass, wood, agriculture crops and glycogen [4]. Biomass hydrolysis by enzymes is a common method for biofuel production, but it has low efficiency and high cost [5]. Many studies have been done on the hydrolysis of biomass to glucose with mineral acids [1, 4, 6], but the large scale use of acid causes several problems such as reactor corrosion, further degradation of monomers, recovery of catalysts, and requires special treatment of the acid residue producing much waste [7].

Solid acid catalysts have various advantages over liquid acid catalysts, such as: simple products separation, possible recycling, and less damage to the reactor [1]. Heteropoly acids (HPAs) are a type of solid acid consisting of transition metal–oxygen anion clusters. HPAs have received much attention due to their fascinating architectures and excellent physicochemical properties, such as Brønsted acidity, high proton mobility and good stability. They dissolve in polar solvents and release H⁺, whose acidic strength is stronger than typical mineral acids like sulfuric acid [8, 9].

Lately, HPAs have been widely used as homogeneous catalysts for biomass conversion. Shimizu *et al.* reported HPAs (H₃PW₁₂O₄₀, H₄SiW₁₂O₄₀) and salts of metal cations (Mn⁺) and PW₁₂O₄₀³⁻(M_{3/n}PW₁₂O₄₀) for selective hydrolysis of cellobiose and cellulose to glucose in an aqueous phase [10]. In that study the glucose yield after 24 h was in the following order: H₃PW₁₂O₄₀ (53 wt. %) > H₄SiW₁₂O₄₀ (51 wt. %) > HClO₄ (42 wt. %) > H₂SO₄ (29 wt. %) > H₃PO₄ (12 wt. %). This indicates

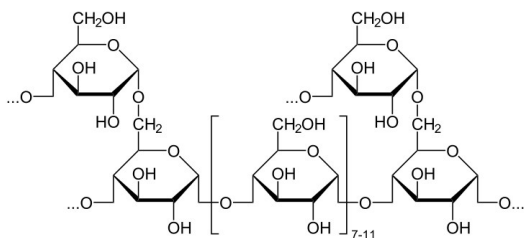
that a stronger Brønsted acid is more favourable for the hydrolysis of a glycosidic bond [10]. Juan *et al.* investigated the potential of H₃PW₁₂O₄₀ for the hydrolysis of cellulose to glucose under hydrothermal conditions. A remarkably high yield of glucose (50.5%) and selectivity higher than 90% at 453 K were found after 2 h [11]. Ogasawara *et al.* showed that highly negatively charged polyanion (H₅BW₁₂O₄₀) promoted efficiently conversion of crystalline cellulose into water-soluble saccharides in concentrated aqueous solutions (82 % total yield and 77% glucose yield, based on reacting cellulose with a 0.7 M H₅BW₁₂O₄₀ solution) [12]. The heteropoly acids could be separated from the homogeneous solution and recycled by extraction with diethyl ether [11], but this process takes a long time, and the extraction is not complete. Some traces of the catalyst remain in the product.

Graphene has received much attention of researchers in the past few years due to its exceptional electronic, mechanical, and optical properties, high surface area, and biocompatibility. It is used in various applications including electrochemical, biosensors [13], transistors for nano-electronics [14], solar cells [15] etc. Because of its excellent adsorptive ability, graphene is also used as support for heterogeneous catalysts. J.M. Yang *et al.* loaded platinum nanoparticles on sulfonated graphene and used it as conductive polymer for fuel-cell applications [16]. S.M. Choi *et al.* synthesized surface-functionalized graphene nanosheets (GNS) with 80 wt. % Pt loading with particle size of less than 3 nm. These Pt/GNS catalysts provided improved mass specific activity in alcohol electro oxidation [17]. Polyoxometalate-graphene composites were recently exploited for super capacitor and electrocatalytic (nitrite electro oxidation) applications [18, 19].

The graphene supported catalysts have also demonstrated high activity in biomass conversion [1, 20]. Supported solid acid catalysts on graphene oxide, and on sulfonated graphene oxide nanosheets have been prepared by Wei *et al.* [21]. The

experimental results indicated that the catalytic activity of the synthesized catalyst was superior to that of other solid acid catalysts and also better than that of H_2SO_4 . They assigned the high activity of the catalyst to the formation of hydrophobic cavities on the graphene sheet containing oxygen groups on its surface. *Kitano et al.* reported on the enhancement of the hydrolysis of β -1,4-glucan on graphene-based amorphous carbon bearing SO_3H , $COOH$, and OH groups. Their results suggested that the synergistic combination of high densities of the functional groups bonded to amorphous carbon causes the efficient hydrolysis of β -1,4-glucan including cellulose [22].

Glycogen, a water soluble polysaccharide of glucose (Scheme 1) is a better feedstock for glucose production than lignocellulosic biomass as it needs no additional pre-treatment. The synthesis of glycogen from CO_2 by photosynthesis and its subsequent hydrolysis to glucose with high selectivity makes glycogen an abundant and renewable feedstock for the production of glucose [23]. Even though, animal remains are the only source of glycogen as of now, currently immense research is going on to produce glycogen from cyano bacteria whereas CO_2 is used as feedstock for glycogen synthesis [24]. Owing to such possibilities, strategies need to be developed for the effective conversion of glycogen to glucose which has been the objective of this study.



Scheme 1: Chemical structure of glycogen, a rich and abundant source of glucose.

The hydrolysis of glycogen to glucose is a critical step in the production of bioethanol and other value added chemicals. In the previous work *Gedanken et al.*, converted glycogen to glucose with HCl and HPA 's as a catalyst. The glucose yields obtained with HCl and $HSiW$ catalysts were 62 and 63 wt. %, respectively [4]. However, the process was corrosive and the products separation after the hydrolysis was time consuming and involved organic solvents [4]. We believe that the development of a new supported catalyst can overcome these disadvantages.

In this article we report on a new catalyst of silico tungstic acid ($HSiW$) supported on graphene ($HSiW/G$). The catalyst preparation was performed by a sonochemical method which has been proven as an effective technique for synthesis of the supported catalysts [25, 26]. The catalytic activity of $HSiW/G$ was studied for the hydrolysis of glycogen. This supported catalyst could be easily separated from the reaction mixture. The physical and chemical properties of the catalysts were studied by the following methods: X-ray diffraction (XRD), transmission electron microscopy (TEM), high resolution scanning electron microscope (HR-SEM), N_2 isothermal adsorption-desorption (Brunauer-Emmett-Teller, BET), FT-IR and Raman spectroscopy, inductively coupled plasma (ICP) analysis, and dynamic light scattering (DLS).

Results and discussion

Catalyst characterization

The morphology of the catalyst $HSiW/G$ was studied by using HR-SEM (Fig. 1).

Sheets with layered structure were observed in the case of commercial graphene (Fig. 1a). The $HSiW/G$ catalyst showed randomly oriented spherical particles of $HSiW$, in the range of 100-250 nm, on the graphene sheets (Fig. 1b). It could be seen that the original smooth surface of graphene was partly changed after deposition of $HSiW$, but the layered structure of graphene was not destroyed. The amount of $HSiW$ on graphene was found to be 2.5 wt. % by ICP analysis.

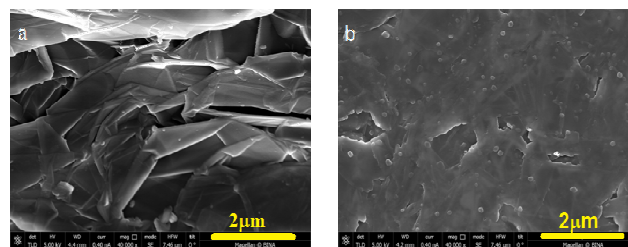


Fig. 1. HR-SEM images of (a) commercial graphene and, (b) graphene coated with $HSiW$ using sonochemical method.

The influence of sonication on the morphology and size of $HSiW$ was studied by TEM and DLS analysis. The TEM image indicated that after 1 h of sonication of $HSiW$ in ethanol without graphene, spherical $HSiW$ nanoparticles were formed with sizes in the range of 100-400 nm (Fig. 2(b)). After the same period (1h) of regular stirring of $HSiW$ in ethanol the spherical particles of slightly larger size in range of 200-500 nm were found. In addition to the large particles, very small particles were also observed in both treatments. The TEM results confirmed that the spherical nanoparticles on the surface of graphene shown in Fig. 1 were indeed $HSiW$.

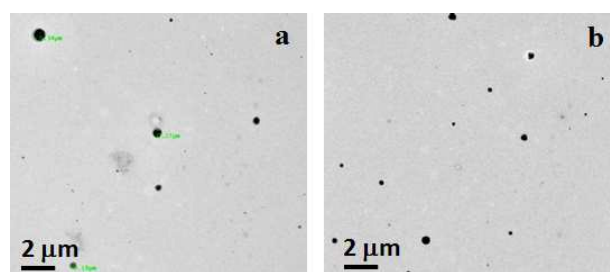


Fig. 2. TEM images of the $HSiW$ after (a) 1 h stirring, and (b) 1 h sonication.

In addition to TEM, DLS analysis was also employed to measure the particle size of $HSiW$ upon different treatments (Fig. 3). The results were in agreement with the TEM images. It was found that with an increase in the sonication time from 15 to 60 min the average particle size decreased from 380 to 340 nm. *Jafari et al.* made similar observations in the reduction of particle size of colloidal nanosilica from 170 to 60 nm as the sonication time is increased from 0.25 to 60 min [27]. Such a reduction of particle size results in improved catalytic performance of $HSiW/G$ in the hydrolysis process.

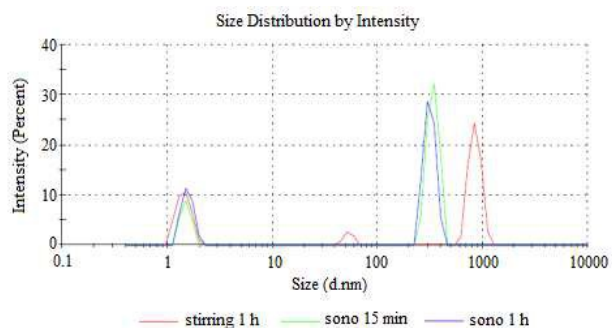


Fig. 3. DLS plot depicting the size distribution of HSiW particles after 15 min sonication, 1 h sonication and 1 h stirring.

The XRD patterns of the commercial graphene and HSiW/G catalyst are shown in Fig. S1. Sharp diffraction peak at $2\theta = 28^\circ$ indicating an interlayer distance of 0.335 nm is typical of graphene (Fig. S1). The XRD results of HSiW/G are similar to those of graphene, which indicates that the HSiW adsorption process does not change the lattice constants of graphene.

The amount of HSiW on graphene (2.5 wt. %) was analyzed by ICP. This loading of HSiW on the catalyst is too low to be detected by XRD. Even with the higher loadings of HSiW (10 wt. %) in the HSiW/G, the XRD pattern did not change. This could be due to the amorphous nature of HSiW on graphene.

The textural properties of HSiW/G catalysts were studied by BET analysis (Table 1).

Table 1. BET measurements

Sample	Surface area [m ² /g]	Average pore radius [Å]	Pore volume [mL/g]
Graphene	73	29	0.11
HSiW/G	52	26	0.07
HSiW	1.8	10	0.009

The BET specific surface area for HSiW supported on graphene with 2.5% loading reached 52 m²/g. The data in Table 1 showed that the specific surface area of the HSiW/G catalysts is reduced by 30% as compared to the commercial graphene. The surface area of pure solid HSiW is only 1.8 m²/g. Thus, the deposition of HSiW on graphene with HSiW led to a better dispersion of active components onto the graphene surface. The pore size and pore volume of the HSiW/G are slightly less compared to the commercial graphene. This could be because of partial blocking of the small graphene pores (diameter \approx 1.2 nm) [28] with the HSiW Keggin (\approx 1.5 nm) units.

The FT-IR spectra of bare graphene, HSiW and HSiW/G catalyst are shown in Fig. 4. As shown before by *P.S. Wate et al.* [29], the FT-IR spectra of graphene did not show any significant absorption peaks over the range of 400-2000 cm⁻¹.

The FT-IR spectrum of HSiW demonstrated four characteristic peaks at 1020, 982, 921, and 798 cm⁻¹ that are assigned to the stretching modes of Si–O, W=O, W–Oe–W, and W–Oc–W, respectively [30].

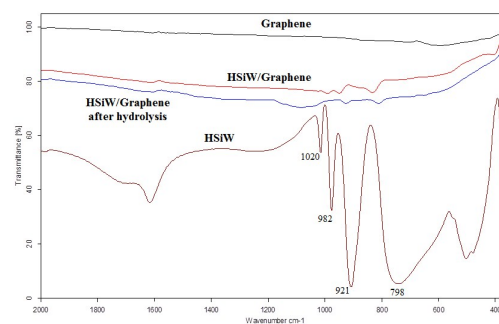


Fig. 4. FT-IR spectra of graphene, HSiW/G and HSiW.

In the spectrum of HSiW/G the peaks in the region of 1020 – 780 cm⁻¹ are very weak and slightly shifted to lower wavelengths. This shift indicates strong interaction between graphene and the catalyst, causing the weakening of the various bonds. A similar effect was observed by *Chen et al.* [30] upon stabilization of HSiW by organic molecules. The FT-IR results clearly demonstrated the fact that HSiW was effectively deposited on graphene and its strong interaction with the support.

The Raman spectra of bare graphene, HSiW and HSiW/G catalyst are shown in Fig. 5.

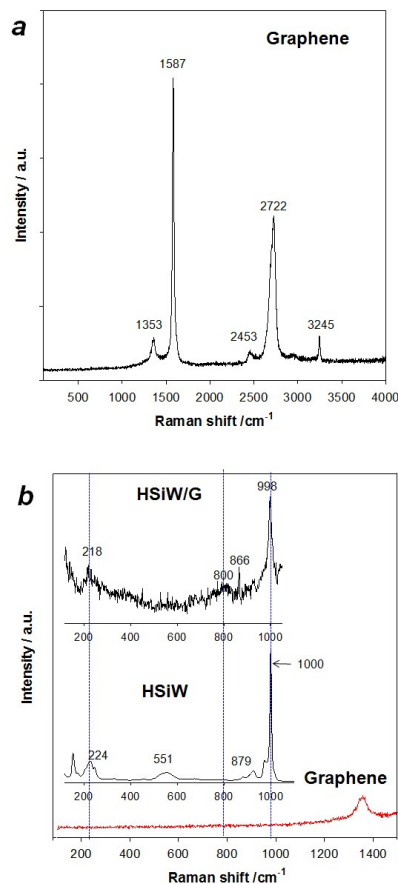


Fig. 5. Raman spectrum of graphene in full range (a), and Raman spectra of graphene, HSiW and HSiW/G (b). Dash blue lines are eye-guides.

The most prominent features in the Raman spectra of graphene are the G-band appearing at 1587 cm⁻¹ and D-band appearing at 1353 cm⁻¹ (Fig. 5a). The G-band represents the

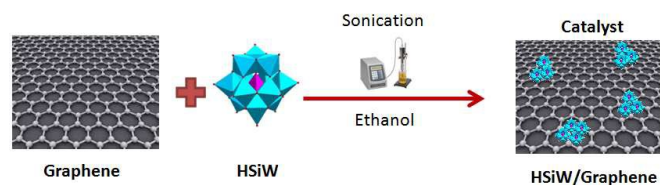
planar configuration sp^2 bonded carbon that constitutes graphene lattice. It is associated with the doubly degenerate (iTO and LO) phonon mode (E_{2g} symmetry). The D-band corresponds to disordered sample or to the edge of a graphene [31, 32].

The Raman spectroscopy technique was used extensively for observing the Keggin structure and also for proving its presence on the graphene [28, 33, 34]. The Raman spectrum of commercial HSiW (Fig. 5b) showing the most intense bands at 1000 cm^{-1} , 974 cm^{-1} , 551 cm^{-1} and 224 cm^{-1} assigned to stretching of $W=O$, bending of $W-Oc-W$, $O-Si-O$, and WO_3 vibrations, respectively. These signals are typical for Keggin structures [28]. In order to study the possible interaction between HSiW and the graphene support we focused on the Raman spectral domain of HSiW (Fig. 5b).

The Raman spectrum of HSiW/G is similar to that of the bare heteropoly acid. The spectrum showed peaks at 998 cm^{-1} , 866 cm^{-1} and 218 cm^{-1} for the $W=O$ stretching, $W-Oc-W$ bending mode, and WO_3 bending, indicating the preservation of the Keggin structure of the HSiW on the surface of graphene. However, a shift in two bending modes is noticed. The $W-O-W$ and WO_3 modes decreased from 879 to 866 cm^{-1} and from 224 to 218 cm^{-1} , respectively. Such a shift might be due to the strong interaction of HSiW with the graphene support, which correlates with the FT-IR result. A similar shift to lower wavenumbers was also observed in Raman spectra of HSiW deposited on Al_2O_3 and SiO_2 [28, 33, 34].

XRD, Raman and SEM studies indicated that the graphene layers are not damaged during sonochemical synthesis of the HSiW/G catalyst. Based on the Raman results it could also be argued that the units of the HSiW were not destroyed during the deposition and they are well dispersed on the surface of graphene. The HSiW is homogeneously distributed on the surface of graphene and strongly anchored to the support. Even after the catalytic hydrolysis of glycogen, the bands corresponding to HSiW were observed in the FT-IR spectra (Fig. 4).

The sonochemical deposition of HSiW on the graphene substrate is presented in Scheme 2.



Scheme 2. Synthesis of HSiW/G catalyst by sonochemical method.

Our explanation of the ultrasound assisted coating is based on the phenomena of cavitation, the formation, growth and implosive collapse of the acoustic bubbles in the liquids. The nanoparticles (NPs) of HSiW created in the liquid under ultrasound waves are thrown to the solid by micro jets and shock waves, which are the after effects of the cavitation collapse [35, 36]. The speed and power of the micro jets is extremely high ($>500\text{ m/sec}$) causing the strong anchoring of the NPs to the surface of the substrate. Low frequency ultrasound has diverse applications. Fang *et al.*, utilized ultrasound for promoting a variety of crucial reactions (dewaxing, removal of impurities, particle size reduction, isolation of chemicals from biomass, delignification, fractionation, reduction of crystallinity and acceleration of

saccharification and fermentation) involved in the conversion of biomass to biofuels [37]. Shewale *et al.* utilized the potential of 20 kHz ultrasound for the particle size reduction of sorghum slurry from 302 to $115\text{ }\mu\text{m}$ (38%) which resulted in improved glucose yield. The particle size reduction was due to the disruption of the protein matrix and the amylose-lipid complexes surrounding the starch granules [38]. Such physical effects that are due to acoustic cavitation were well documented [39].

Glycogen hydrolysis under hydrothermal reaction conditions

The glycogen hydrolysis was carried out under hydrothermal conditions in an autoclave. ^{13}C NMR spectra of the products obtained with three types of catalysts (bare HSiW, bare graphene and HSiW/G) are shown in Fig. 6.

As suspected, no glycogen conversion was observed when only graphene was used as catalyst (Fig. 6a). With HSiW, complete conversion of glycogen to glucose (60.3 (C6), 69.2 (C4), 72.4 (C2), 73.7 (C3), 75.3 (C5), 92 (C1 α) and 95.3 (C1 β)) was obtained (Fig. 6c). With the HSiW/G catalyst, in addition to glucose, some traces of unreacted glycogen (60.6 , 69.4 , 71.2 , 71.6 , 71.8 , 73.4 , 76.8 , 99.6 ppm) were also noticed (Fig. 6b), indicating that the hydrolysis is not complete. This fact can be explained because of the low content of the HSiW in the catalyst. According to ICP analysis, the content of HSiW in HSiW/G catalyst was found as 2.5 wt. \% . In other words, the amount of HSiW in 0.1 g HSiW/G catalyst used for the hydrolysis reaction is 0.0025 g . It is interesting to note that even at such a low loading of the solid acid, the synthesized catalyst is effective for the hydrolysis of glycogen. In addition, under the reaction conditions used, the hydrolysis of glycogen was selective. No by-products, such as hydroxymethyl furfural (HMF), levulinic acid and formic acid were formed. When the hydrolysis of glycogen was previously performed with HCl in microwave, these by-products were observed [4].

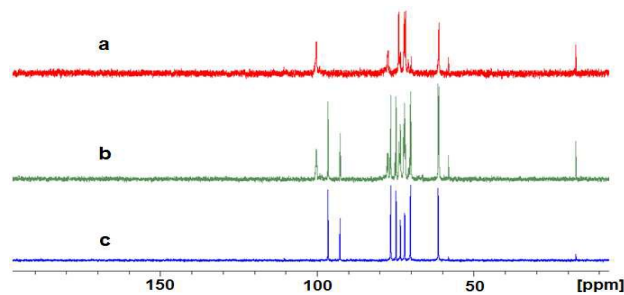


Fig. 6. ^{13}C NMR spectra of hydrolyzate obtained with (a) bare graphene, (b) HSiW/G and (c) HSiW (reaction conditions: 0.1 g glycogen; 0.1 g catalyst; 2 mL water; $100\text{ }^\circ\text{C}$; 1 h).

For optimizing the glycogen hydrolysis process with HSiW/G and detailed studying, the reaction was performed in a larger reaction batch of 20 mL under different time, temperature, and ratio of HSiW/G to glycogen. The products obtained at various reaction conditions were analyzed by HPLC analysis, and the results are presented in Fig. 7.

A representative HPLC chromatogram recorded on the hydrolyzate obtained from the hydrolysis of glycogen is shown in Fig. S2. The retention time was detected in control experiments with different amounts of glucose. The peak with a retention time of 12.3 min is attributed to glucose.

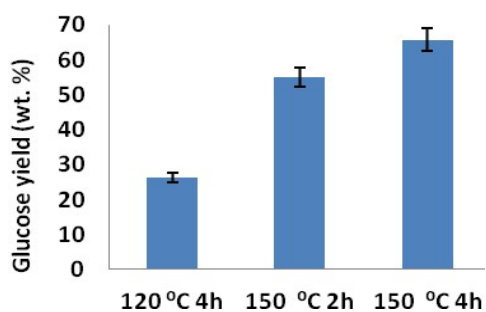


Fig. 7. Glucose yield (wt. %) from glycogen hydrolysis as a function of reaction time and temperature (reaction conditions: 1 g glycogen; 1 g HSiW/G catalyst; 20 mL water).

After 2h at 120 °C no glucose was found. The absence of glucose at 120 °C in the series of experiments with large batch (20 mL) comparing to the formation of glucose at 100 °C with the small batch (2 mL) is, probably, due to the higher volume needs longer time and higher temperature to get the proper pressure in the vessel compared to the one used with small batch. When the reaction time was increased at the same temperature, the yield of glucose was 26 wt. % (Fig. 7).

At 150 °C after 2 h the yield of glucose was 55 wt. %. Prolonging of the reaction time to 4h increased the glucose yield to 66 wt. %. It is clear that higher temperatures lead to higher product yields. As a result, the duration time of 4h at 150 °C was chosen to be the optimal conditions with the highest yield of glucose.

The weight ratio of the catalyst (HSiW/G) to glycogen was varied in range 1÷0.25. The yields of glucose generated from hydrolysis of glycogen with various amounts of catalyst are depicted in Fig. 8.

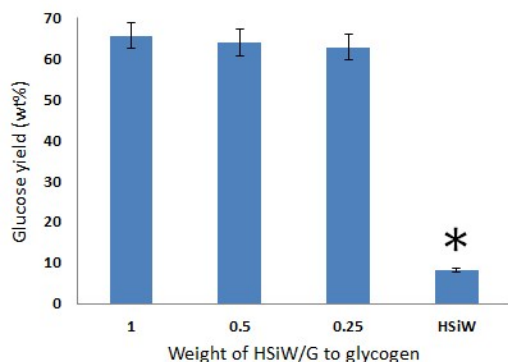


Fig. 8. Glucose yield from glycogen hydrolysis at different weight ratios of HSiW/G to glycogen (glycogen- 1 g; HSiW/G- 1, 0.5 and 0.25 g; time- 4h; temperature 150 °C).

* bare HSiW– 0.025 g (this corresponds to the amount of HSiW present in the HSiW/G catalyst at ratio of HSiW/G to glycogen 1:1).

It was observed that at a hydrolysis temperature of 150 °C for 4 h, the yield of glucose for all of the examined ratios of HSiW/G to glycogen (1:1; 0.5:1 and 0.25:1) was almost the same (65 wt. %). When same amount of bare HSiW as that present in the supported catalyst (HSiW/G) was used as a catalyst, the glucose yield was dramatically low (8.2%). Thus,

the bare HSiW is about 8 times less active than HSiW deposited on graphene. The increase of catalytic activity of the supported HSiW compared to the bare HSiW could be due to the effective and uniform distribution heteropoly acid on the surface of graphene. Moreover, HSiW/G catalyst has a larger specific surface area ($52 \text{ m}^2\text{g}^{-1}$) compared to bare HSiW ($1.8 \text{ m}^2\text{g}^{-1}$). The large surface area enables effective contact between the uniformly distributed acid sites on the graphene surface and the glycogen that promotes rapid, effective and efficient catalytic reaction.

The observed enhanced activity of HSiW/G could be due to the strong binding of the heteropoly anions to the aromatic π -cloud on graphene surface (similar to π - π interactions) leading to higher accessibility of the protons for the cleavage of the glycosidic bond in glycogen. Kim *et al.*, reported such strong electrostatic interactions between polyoxometalate and rGO [18]. In contrast, in the case of bare HSiW, the protons of the poly anion are freely rotating in the reaction medium and are in constant motion. As a result, the probable interaction between the protons and the reactant (glycogen) is low, resulting in lower yields of glucose.

We have further evaluated the stability of HSiW/G in the hydrolysis of glycogen. After the first run under optimal hydrothermal conditions (1 g HSiW/G, 1 g glycogen, 20 mL water, 150 °C, 4h) the HSiW/G was separated from the aqueous product mixture by centrifugation. The collected catalyst was dried in vacuum overnight and subsequently reused for the second and third runs under identical reaction conditions. The results, as measured by HPLC analysis are presented in Fig. 9.

The glucose yield after three reaction cycles was still high (63.3 wt. %) indicating that HSiW can be reused without loss in catalytic activity. Even after three repeated runs, the amount of HSiW on graphene was found to be 2.2 wt. %. This indicates that the catalyst is not just a physical mixture but a supported system wherein the active component (HSiW) is strongly adhered to the support (graphene). The good catalyst stability could be due to the use of sonochemical deposition method which leads to the strong adherence of HSiW to the support [40, 41]. The catalyst can serve also in a hydrothermal flow system, since the HSiW will not leach out easily.

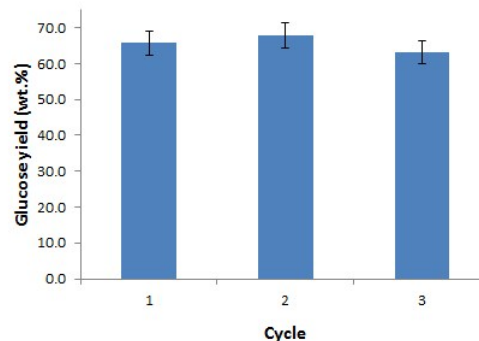


Fig. 9. Recyclability of the HSiW/G catalyst in the hydrolysis of glycogen. (reaction conditions: 1 g of glycogen ; 1 g of the solid acid catalyst; 20 mL of H₂O; 150 °C; 4h). The catalyst was recovered by 9000 rpm centrifugation for reuse.

It is difficult to explain the excellent catalytic activity of HSiW/G in the hydrolysis of glycosidic bond due only to the higher surface area and homogenous deposition of HSiW on the graphene surface. Wei *et al.* attributed the excellent catalytic activity of sulfonated graphene oxide (sGO) in the hydrolysis of

cellobiose and isoflavones to the interaction between the anions of the side chains of the catalyst and the reactants. In addition to hydrophilic groups, sGO has hydrophobic, flexible graphene sheets that can help to form hydrophobic cavities on the graphene surface. This adsorbent microregion has affinity for certain reactants [21].

We suppose that the mechanism of interaction between HSiW/G and glycogen was similar to the one discussed in [21]. Namely, the hydrophobic graphene sheets of HSiW/G first provide hydrophobic cavities to the glycogen on the surface of the catalyst. Then the hydrophobic parts (carbon rings) of the glycogen are encapsulated by the graphene, and the hydrophilic parts (OH and O) form hydrogen bonds with the heteropoly acid on the graphene surface. In addition, to the H⁺ and different metal-oxygen bonds, the heteropoly acid inherently contains water molecules within the crystal structure that contribute to the hydrophilic nature of the catalyst. A combination of hydrophilic and hydrophobic regions on the catalyst surface leads to increased concentration of glycogen on the catalyst surface and their by contributes to the enhancement of hydrolysis rate and selectivity. Afterwards, the protons ionized from support catalyst attack the glycosidic bond and catalyze the hydrolysis of glycogen. Finally, the glycosidic bond is broken owing to the hydrolysis of the reactant.

Therefore, the catalyst is a prospectively, selective, and efficient for biomass hydrolysis. Moreover, the usefulness of the catalyst was tested for the hydrolysis of cellulose under the optimal reaction conditions (4 h, 150 °C). A glucose yield value of 33 wt. % was obtained, indicating the activity of the catalyst (HSiW/G) for cellulose hydrolysis. So, the catalyst designed could be used for the hydrolysis of cellulosic biomass. Shimizu *et al.* reported a glucose yield value of 15 % in a H₃PW₁₂O₄₀ catalyzed cellulose hydrolysis process under hydrothermal conditions (150 °C, 2 h). Moreover, prior the hydrolysis process, the cellulose was pretreated for 48 h under ball milling [10]. Tian *et al.*, reported a glucose yield value of 50.5 wt. % from the hydrolysis of cellulose in the presence of H₃P₁₂O₄₀ catalyst under hydrothermal conditions (180 °C; 3 h) [11]. A high glucose yield value of 75.6 wt. % was reported by Li *et al.*, from the hydrolysis of cellulose under microwave irradiation using conc. H₃PW₁₂O₄₀ as catalyst [42]. The above comparison with the recent reports on cellulose hydrolysis clearly indicates the advantage of the current process being based on the use of a heterogeneous catalyst unlike the homogenous nature of the catalyst reported [10, 11, 42]. Even under modest hydrolysis conditions glucose yield values of 33 and 66 wt. % were respectively obtained from cellulose and glycogen using the HSiW/G catalyst.

For comparing the effect of catalyst preparation method on its activity, glycogen hydrolysis was also carried out under identical reaction conditions, using the HSiW/G catalyst prepared by the impregnation method. A glucose yield value of 40 wt. % was observed relative to the value of 66 wt. % that was obtained using the catalyst prepared by the sonochemical route. In addition, the hydrolyzate was found to be acidic (pH 1-2) in the case of impregnation based catalyst unlike the near neutral (pH 6) nature of the hydrolyzate generated using sonochemical based catalyst. This result indicates strong interaction between the HSiW and graphene in the catalyst prepared by the sonochemical method.

Experimental

Materials

Tungstosilicic acid hydrate (H₄SiW₁₂O₄₀ nH₂O, HSiW, 99%), Cellulose powder (Avicel® PH-101; ~50 μm particle size) and glycogen from bovine liver were purchased from Sigma-Aldrich Co., (St. Louis, MO, USA). The graphene nano platelets (6-8 nm thick x15 microns wide) were purchased from STREM chemicals, Newburyport, MA, USA. The chemicals were used without further purification.

Catalyst preparation

An ultrasound-assisted method was used to prepare the supported HSiW/G catalysts. Typically, the following procedure was follows: 2 g HSiW was first dissolved in 80 mL ethanol, followed by the addition of 2 g graphene. Owing to easy evaporation, ethanol is used as a solvent. The synthesis was performed in the glass beaker reactor of 120 mL volume. The mixture was sonochemically irradiated with 1 cm² titanium horn immersed 1 cm into the solution for 1 h with an efficiency of 40% (amplitude) with no external cooling (Sonicator 20 kHz, Sonics & Materials, VCX-750). After 1 h the temperature of the reaction slurry was 60 °C. The product was then collected by centrifugation and dried in vacuum overnight.

In addition to the sonochemical route, conventional impregnation method was also used for the preparation of HSiW/G catalyst. The catalyst preparation process in the conventional impregnation method comprise of dissolving 2 g HSiW in 80 mL ethanol, followed by the addition of 2 g graphene. The mixture was put for 4 h stirring. Then the solvent was evaporated using water bath followed by drying of the catalyst in vacuum overnight. The catalysts prepared in the two afore mentioned routes were compared in the glycogen hydrolysis reaction.

Catalyst characterization

The XRD analysis of the HSiW/G was performed on a Bruker D8 diffractometer with Cu Ka-1.541 Å radiation. Morphology and texture of the HSiW on the graphene were studied by transmission electron microscopy (TEM) JEOL jem-1400 (120 kV) and scanning electron microscopy (HR-SEM), FEI company TM MAGELLAN 500L (Holland). The particles size distribution of HSiW (dispersed in ethanol) was estimated by the DLS method using a Malvern Zetasizer Nanoseries device (Malvern Instruments, Malvern, UK). The amount of HSiW deposited on graphene by sonication was determined by the inductive coupled plasma (ICP) method on the ULTIMA JY 2501 instrument. Surface area, pore volume and pore size distribution were measured using a Nova 3200e Quantachrome analyzer. The surface area was calculated from the linear part of the BET plot. Pore size distribution was estimated using the Barrett–Joyner–Halenda (BJH) model with the Halsey equation, and the pore volume was measured at the P/P0 0.9947 signal point.

Fourier transform reflection infrared (FT-IR) spectra were obtained using a FT-IR spectroscopy (Bruker Tensor 27). Raman spectra were collected using the Renishaw inVia Raman microscope equipped with Leica DM2500 M analysis microscope Leica Microsystems), sample focusing was done by a 50X (N.A 0.75) lens. All the samples were irradiated by a 514 nm excitation wavelength with a constant power of ~0.25 mW. The imaging.

Glycogen hydrolysis reaction

For glycogen hydrolysis process a stainless steel home-made autoclave 50 mL volume was used. Typically, 1 g glycogen and 1 g catalyst were dispersed in 20 mL water and placed into the autoclave. The autoclave was then placed in a regular air oven for the hydrothermal treatment of glycogen. Reaction parameters such as time, temperature of heating, weight ratio of catalyst and glycogen were varied to optimize the hydrolysis process. In addition to glycogen, cellulose was also tested as carbohydrate feedstock for glucose production.

The reusability of catalyst was investigated. After the reaction, the catalyst was separated from the solution by centrifugation and dried in vacuum overnight. The catalyst was used for a second run without regeneration under identical hydrothermal reaction conditions. The process was repeated 3 times.

The progress of the glycogen hydrolysis reaction was monitored using ^{13}C NMR spectroscopic analysis on a Bruker Avance DPX 300 instrument. D_2O was used as a solvent.

The water soluble products of catalyzed hydrolysis reactions were analyzed by HPLC (Merck-Hitachi LaChrom System L-7000 equipped with L-7455 Diode Array Detector and Schambeck SFD RI 2000 Refractive Index Detector, Bad Honnef, Germany). Analyses carried out using Rezex-ROA ion exclusion chromatography column 300x7.8 mm (Torrance, CA, USA) equipped with a matching guard column. The mobile phase used was 0.005N H_2SO_4 under isocratic elution for 45 min at a flow rate of 0.5 mL/min at ambient temperature, with injection volume of 10 μL . EZ Chrom Elite v. 3.1.7 software was used for data acquisition and processing, with RI signal acquired using external analog input. The content of the glucose in the hydrolyzate was calculated using a calibration curve obtained from a series of external glucose standards.

Conclusions

Polyoxometalate (HSiW) was deposited on the surface of graphene by the sonochemical method. Physico-chemical characterization of HSiW/G catalyst was done using SEM, TEM and XRD which demonstrated a homogeneous distribution of HSiW on the surface of graphene support. The catalytic performance of the synthesized catalyst was evaluated for the hydrolysis of the glycosidic bond of glycogen to glucose. The following conclusions have been drawn: the catalytic activity of HSiW/G is significantly higher than that of the bare HSiW. The hydrolysis process with HSiW/G is selective, fast and green with high yield of glucose (66 wt. %). The sonochemical method provided strong anchoring of HSiW to graphene and high stability of the catalyst. The reuse of HSiW/G catalyst in 3 cycles was demonstrated. The glucose yield after three reaction cycles was not altered significantly, showing that HSiW/G is a reusable, economically viable and green catalyst.

Acknowledgements

We thank the Israel Science Foundation for supporting this research by grant 12/586, and to the Ministry of Science and Technology for the research grant 3-9802.

Notes and References

^a Department of Chemistry and the Center for Advanced Materials and Nanotechnology, Bar Ilan University, Ramat Gan, 52900 Israel. gedanken@mail.biu.ac.il.

^b The Mina and Everard Goodman Faculty of Life Sciences, Bar Ilan University, Ramat Gan, 52900 Israel.

^c Department of Materials Science & Engineering, National Cheng Kung University, Tainan 70101, Taiwan.

† Electronic Supplementary Information (ESI) available: Typical HPLC chromatogram of the hydrolyzate (hydrothermal heating of 1 g glycogen and 1 g HSiW/G in 20 mL water, 150 °C, 4 h).

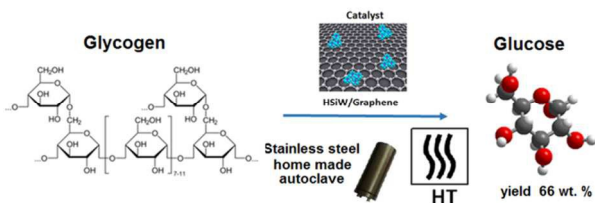
- 1 Y. B. Huang and Y. Fu, *Green Chem.*, 2013, **15**, 1095.
- 2 J. P. Lange, E. Heide, J. Buijtenen and R. Price, *ChemSusChem.*, 2012, **5**, 150.
- 3 J. R. Regalbuto, *Science*, 2009, **325**, 822.
- 4 M. Klein, I. N. Pulidindi, N. Perkas, E. Meltzer-Mats, A. Gruzman and A. Gedanken, *RSC Adv.*, 2012, **2**, 7262.
- 5 G. Brodeur, E. Yau, K. Badal, J. Collier, K. B. Ramachandran and S. Ramakrishnan, *Enzyme Res.*, 2011, **2011**, 1.
- 6 I. N. Pulidindi, B.B. Kimchi and A. Gedanken, *Renew. Energy*, 2014, **71**, 77.
- 7 J. Tian, J.H. Wang, S. Zhao, C.Y. Jiang, X. Zhang and X.H. Wang, *Cellulose*, 2010, **17**, 587.
- 8 I. V. Kozhevnikov, *J. Mol. Catal. A: Chem.*, 2009, **305**, 104.
- 9 J. Macht, M. J. Janik, M. Neurock and E. Iglesia, *Angew. Chem. Int. Ed.*, 2007, **46**, 7864.
- 10 K. Shimizu, H. Furukawa, N. Kobayashi, Y. Itaya, and A. Satsuma, *Green Chem.*, 2009, **11**, 1627.
- 11 J. Tian, J. Wang, S. Zhao, C. Jiang, X. Zhang and X. Wang, *Cellulose*, 2010, **17**, 587.
- 12 Y. Ogasawara, S. Itagaki, K. Yamaguchi and N. Mizuno, *ChemSusChem.*, 2011, **4**, 519.
- 13 Z. Wang, F. Li, J. Xia, L. Xia, F. Zhang, S. Bi, G. Shi, Y. Xia, J. Liu, Y. Li and L. Xiam, *Biosens. Bioelectron.*, 2014, **61**, 391.
- 14 P. J. Wessely and U. Schwalke, *Appl. Surf. Sci.*, 2014, **29**, 83.
- 15 L. Kavan, J. Yum and M. Graetzel, *Phys. Status Solidi B*, 2013, **250**, 2643.
- 16 J. M. Yang, S. A. Wang, C. L. Sun and M. D. Ger, *J. Power Sources*, 2014, **254**, 298.
- 17 S. M. Choi, M. H. Seo, H. J. Kim and W. B. Kim, *Carbon*, 2011, **49**, 904.
- 18 Y. Kim and S. Shanmugam, *ACS Appl. Mater. Interfaces*, 2013, **5**, 12197.
- 19 Z. Cui, C. X. Guo, W. Yuan and C. M. Li, *Phys. Chem. Chem. Phys.*, 2012, **14**, 12823.
- 20 D. Verma, R. Tiwari and A. K. Sinha, *RSC Adv*, 2013, **3**, 13265.
- 21 Z. Wei, Y. Yang, Y. Hou, Y. Liu, X. He and S. Deng, *ChemCatChem.*, 2014, **6**, 2354.
- 22 M. Kitano, D. Yamaguchi, S. Suganuma, K. Nakajima, H. Kato, S. Hayashi and M. Hara, *Langmuir*, 2009, **25**, 5068.
- 23 S. Aikawa, Y. Izumi, F. Matsuda, T. Hasunuma, J. S. Chang and A. Kondo, *Bioresour. Technol.*, 2012, **108**, 211.
- 24 S. Aikawa, A. Joseph, R. Yamada, Y. Izumi, T. Yamagishi, F. Matsuda, H. Kawai, J-S. Chang, T. Hasunumabch and A. Kondo, *Energy Environ. Sci.*, 2013, **6**, 1844.
- 25 N. Perkas, P. Gunawan, G. Amirian, Z. Wang, Z. Zhong and A. Gedanken, *Phys. Chem. Chem. Phys.*, 2014, **16**, 7521.

- 26 N. Perkas, J. Teo, S. Shen, Z. Wang, J. Highfield, Z. Zhong and A. Gedanken, *Phys. Chem. Chem. Phys.*, 2011, **13**, 15690.
- 27 V. Jafari, A. Allahverdi and M. Vafaei, *Advanced Powder Technol.*, 2014, **25**, 1571.
- 28 H. Atia, U. Armbrusterb and A. Martin, *J. Catal.*, 2008, **258**, 71.
- 29 P. S. Wate, S. S. Banerjee, A. Jalota-Badhwar, R. R. Mascarenhas, K.R. Zope, J. Khandare and R. D. K. Misra, *Nanotechnology*, 2012, **23**, 415101.
- 30 J. Chen, X. Fang, X. Duan, L. Ye, H. Lin and Y. Yuan, *Green Chem.*, 2014, **16**, 294.
- 31 J. Hodkiewicz, *Thermo Fisher Scientific Inc. Application Note*, 51946, **2010**, 1.
- 32 L. M. Malard, M. A. Pimenta, G. Dresselhaus and M. S. Dresselhaus, *Phys. Rep.*, 2009, **473**, 51.
- 33 S. Zhu, Y. Zhu, X. Gao, T. Moa, Y. Zhu and Y. Li, *Bioresource Technol.*, 2013, **130**, 45.
- 34 N. Legagneux, J. M. Basset, A. Thomas, F. Lefebvre, A. Goguet, J. Sa and C. Hardacre, *Dalton T.*, 2009, **12**, 2235.
- 35 A. Gedanken, *Ultrason. Sonochem.*, 2004, **11**, 47.
- 36 A. Gedanken, *Ultrason. Sonochem.*, 2007, **14**, 418.
- 37 J. Luo, Z. Fang and R.L. Jr Smith, *Prog. Energy Combust Sci.*, 2014, **41**, 56.
- 38 S.D. Shewale and A.B. Pandit, *Carbohydr. Res.*, 2009, **344**, 52.
- 39 I. N. Pulidindi and A. Gedanken, Chapter 6, in *Springer Book Series Production of Biofuels and Chemicals: Ultrasound*, Editors: Z. Fang, L.s. Fan, J. R. Grace, Y. Ni, N. R. Scott and R. L. Smith Jr., 2015, p. 159.
- 40 V. G. Pol, D. N. Srivastava, O. Palchik, V. Palchik, M. A. Slifkin, A. M. Weiss and A. Gedanken, *Langmuir*, 2002, **18**, 3352.
- 41 I. Perelshtein, E. Ruderman, N. Perkas, T. Tzanov, J. Beddow, E. Joyce, T. J. Mason, M. Blanes, K. Moll, A. Patlolla, A. I. Frenkel and A. Gedanken, *J. Mater. Chem. B.*, 2013, **1**, 1968.
- 42 X. Li, Y. Jiang, L. Wang, L. Meng, W. Wang and X. Mu, *RSC Adv.*, 2012, **2**, 6921.

Table of Content

Sonochemical Synthesis of HSiW/Graphene Catalyst for Enhanced Biomass Hydrolysis

Miri Klein, Alexander Varvak, Elad Segal, Boris Markovsky, Indra Neel Pulidindi, Nina Perkas and Aharon Gedanken



Graphene supported silico-tungstic acid catalyst was synthesized sonochemically. Glucose yield was dramatically increased by reusable HSiW/G in the biomass hydrolysis.